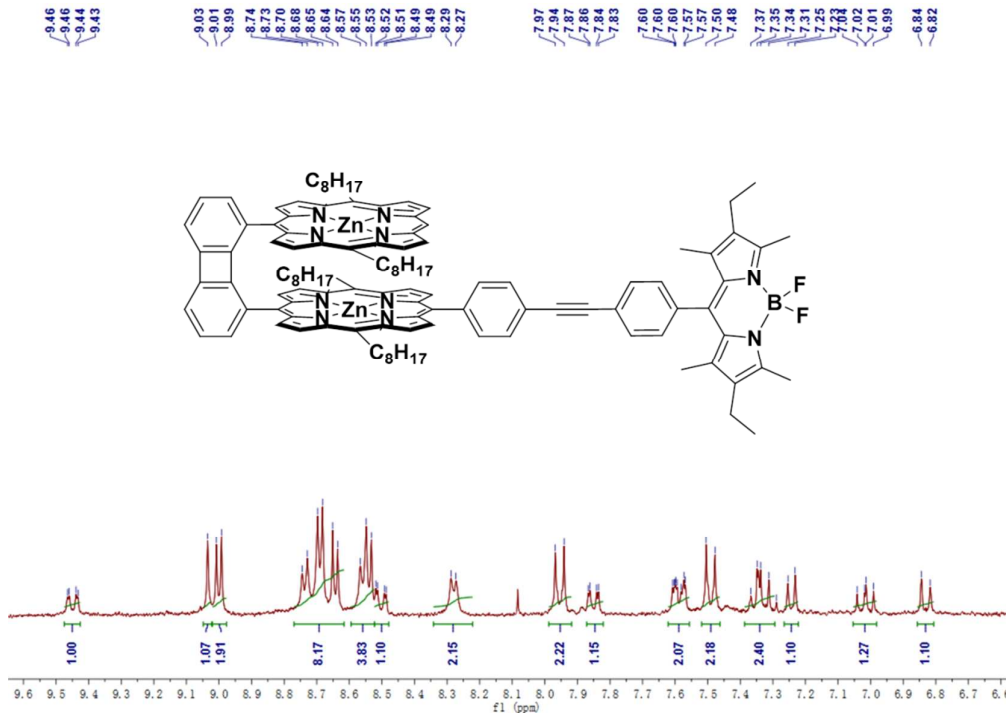
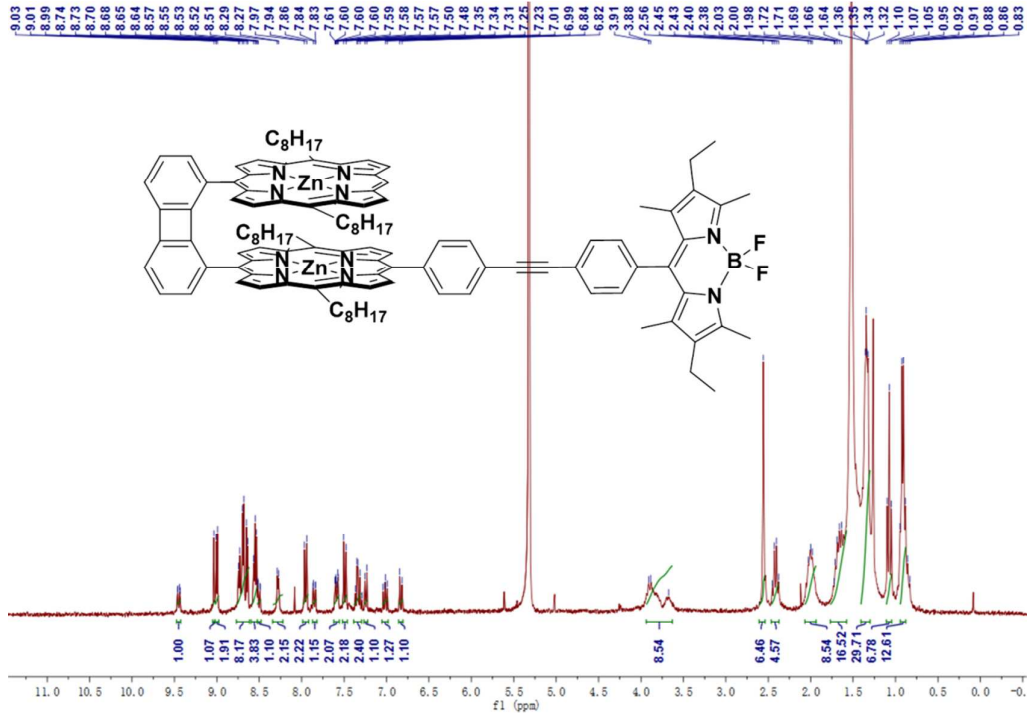


Is π -Stacking Prone to Accelerate the Singlet-Singlet Energy Transfers?

Di Gao, Shawkat M. Aly, Paul-Ludovic Karsenti, and Pierre D. Harvey*

Departement de chimie, Université de Sherbrooke, Sherbrooke, QC, Canada J1K 2R1

Figure S1. ^1H NMR spectrum of 1 in CD_2Cl_2	S2
Figure S2. ^1H NMR spectrum of 1 in CD_2Cl_2	S2
Figure S3. ^1H NMR spectrum of 2 in CD_2Cl_2	S3
Figure S4. ^1H NMR spectrum of 3 in CDCl_3	S3
Figure S5. High resolution MALDI-TOF mass spectrum of 1	S4
Figure S6. MALDI-TOF mass spectrum of 2	S4
Figure S7. MALDI-TOF mass spectrum of 3	S5
Figure S8. Bar graph reporting the calculated oscillator strength and calculated position of the 100 st electronic transitions calculated by TDDFT for 1 (bar graph; f = computed oscillator strength). The black line is generated by assigning a thickness of 1000 cm^{-1} to each bar.	S8
Figure S9. Comparison of $k_{\text{ET}}(S_1)$ for various literature dyads: D12 , D13 , D14 , D15 and D16 at 298 K. Note that these dyads do not bare methyl groups at the β -position of [bod].	S9
Figure S10. Description of the Förster's theory.....	S10
Figure S11. Description of the Dexter's theory	S10
Table S1. Calculated position, oscillator strength (f) and major contributions of the first 100 singlet-singlet electronic transitions for 1	S6
References	S10



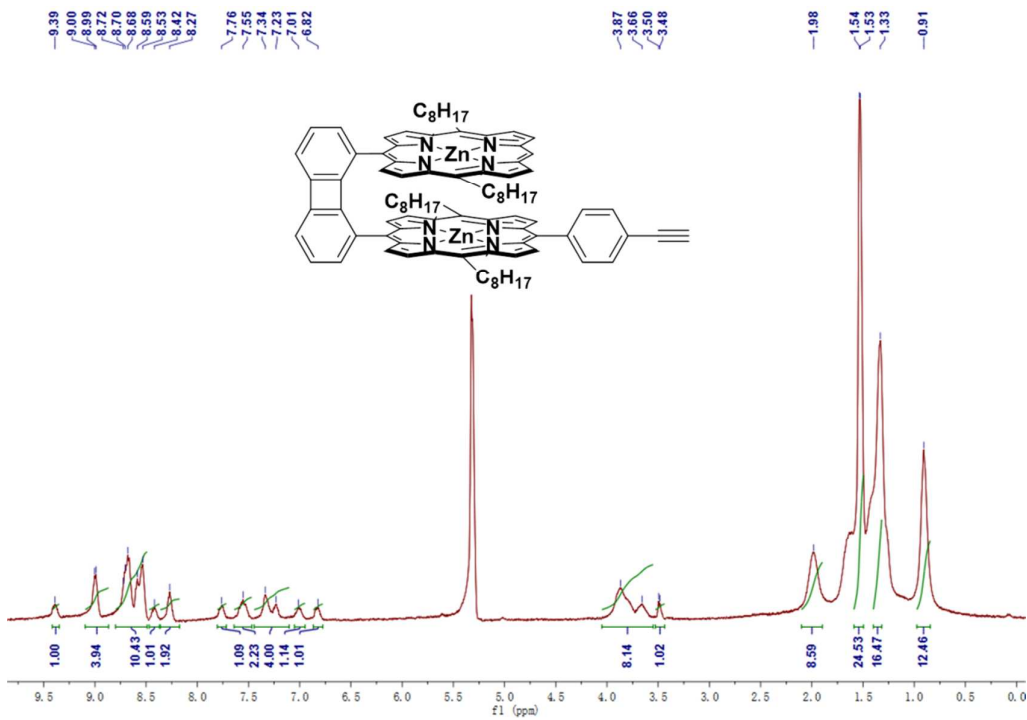


Figure S3. ^1H NMR spectrum of **2** in CD_2Cl_2 .

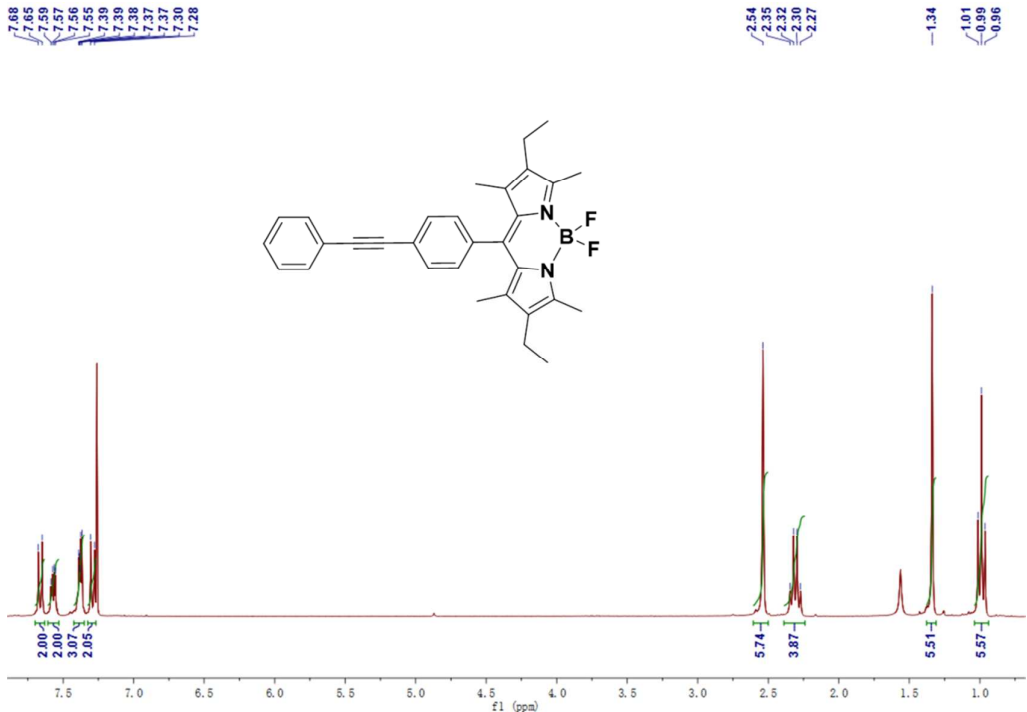


Figure S4. ^1H NMR spectrum of **3** in CDCl_3 .

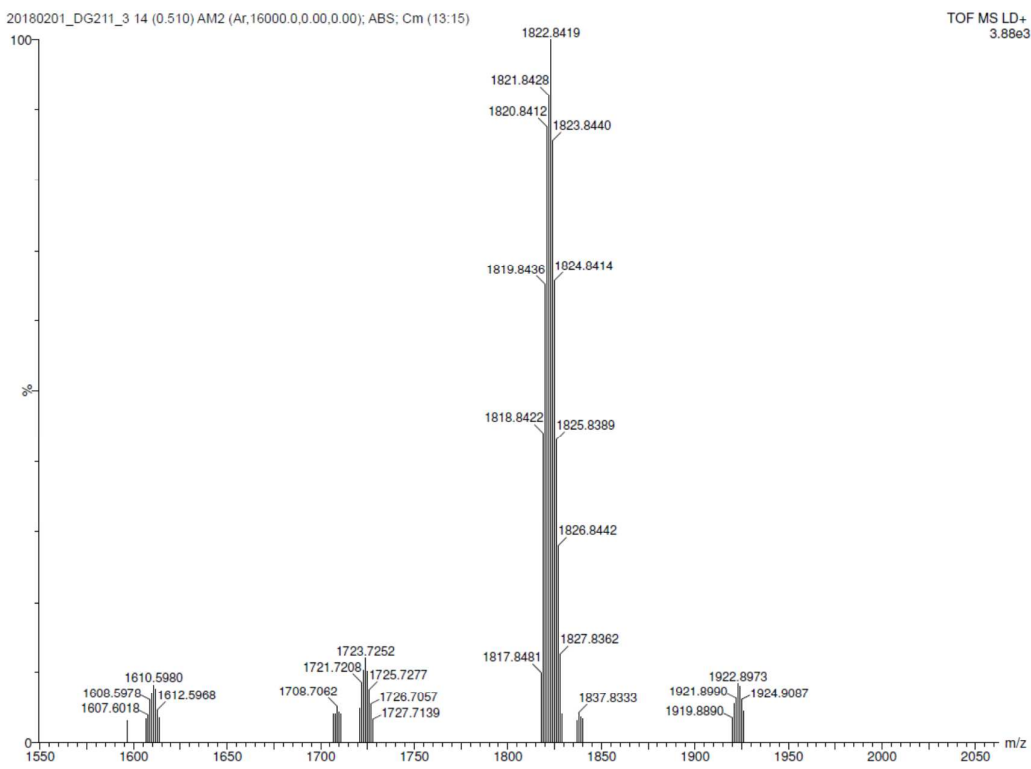


Figure S5. High-resolution MALDI-TOF mass spectrum of **1**.

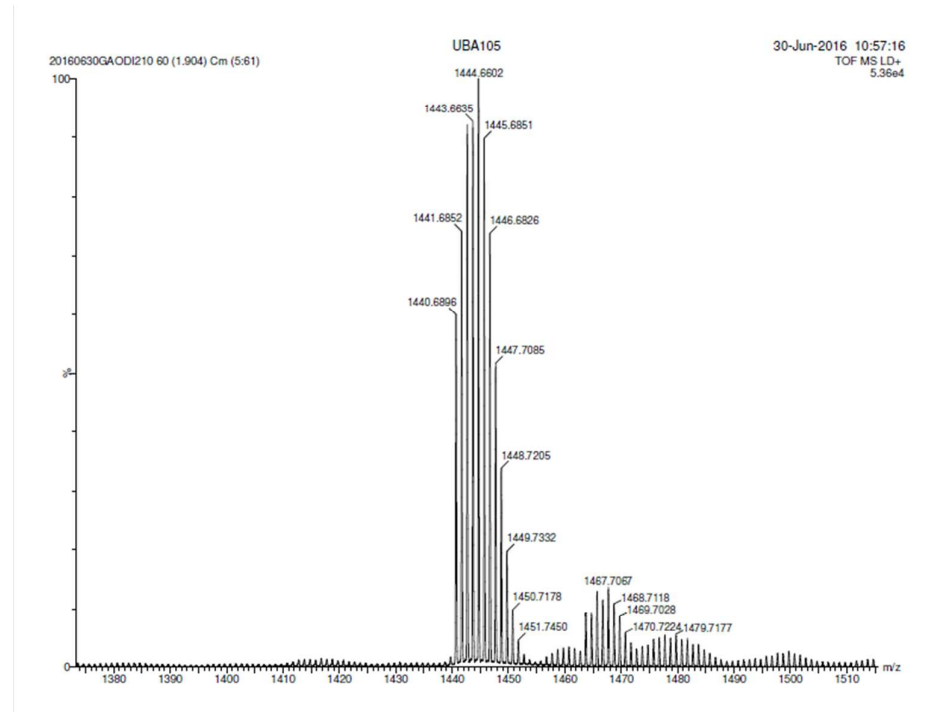


Figure S6. MALDI-TOF mass spectrum of **2**.

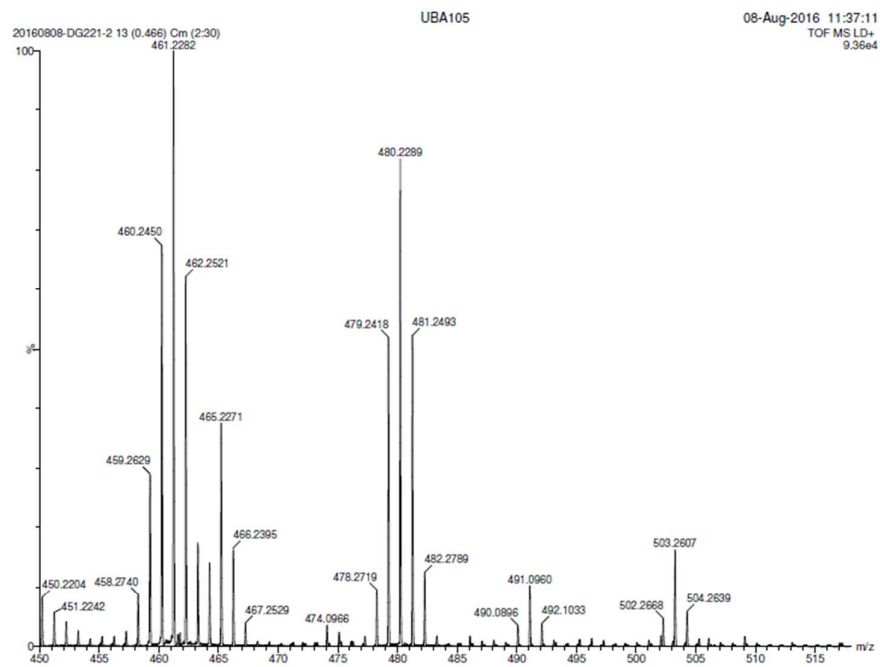


Figure S7. MALDI-TOF mass spectrum of **3**.

Table S1. Calculated position, oscillator strength (f) and major contributions of the first 100 singlet-singlet electronic transitions for **1**.

No.	Wavelength (nm)	Osc. Strength	Major Contribs (%)
1	553.0	0.0467	HOMO→L+1 (65)
2	549.4	0.0057	H-2→L+1 (10), H-1→L+1 (28), HOMO→L+2 (44)
3	543.0	0.0018	H-2→L+3 (10), H-1→L+1 (10), H-1→L+2 (32), HOMO→L+3 (18)
4	539.0	0.0009	H-3→L+1 (12), H-2→L+2 (10), H-1→L+1 (12), H-1→L+2 (10), H-1→L+3 (20), HOMO→L+4 (11)
5	535.2	0.0009	H-1→L+1 (38), HOMO→L+2 (29), HOMO→L+3 (14)
6	528.1	0.0038	H-1→L+2 (14), H-1→L+3 (26), HOMO→L+3 (31)
7	523.9	0.0043	H-1→L+4 (11), HOMO→L+4 (57)
8	520.2	0.0065	H-1→L+3 (17), H-1→L+4 (43)
9	516.5	0.0001	HOMO→LUMO (100)
10	506.8	0	H-1→LUMO (100)
11	494.4	0.0055	H-3→L+1 (36), H-2→L+1 (41)
12	487.1	0.0054	H-3→L+2 (21), H-3→L+3 (30), H-2→L+2 (31)
13	484.1	0.0016	H-3→L+2 (23), H-3→L+3 (13), H-2→L+2 (11), H-2→L+3 (11), H-2→L+4 (29)
14	480.9	0.0098	H-3→L+4 (38), H-2→L+3 (26), H-2→L+4 (13)
15	474.1	0	H-2→LUMO (99)
16	465.4	0	H-3→LUMO (99)
17	431.5	0.1868	H-5→L+1 (24), H-4→LUMO (44)
18	431.2	0.3139	H-5→L+1 (30), H-4→LUMO (33)
19	429.4	0.0591	H-4→LUMO (10), H-4→L+1 (85)
20	426.0	0.0674	H-5→L+1 (25), H-5→L+2 (45)
21	422.0	0.1628	H-5→L+2 (27), H-5→L+3 (24), HOMO→L+5 (19)
22	421.0	0	H-4→L+2 (99)
23	416.3	0.1142	H-5→L+3 (60), HOMO→L+5 (22)
24	415.5	0	H-4→L+3 (99)
25	410.1	0.0001	H-4→L+4 (99)
26	408.8	0.0277	H-5→L+4 (75)
27	405.7	0.0352	H-5→L+4 (15), HOMO→L+5 (19), HOMO→L+6 (21)
28	404.6	0.0181	H-5→L+2 (10), H-1→L+6 (11), HOMO→L+5 (18)
29	404.1	0.0004	H-5→LUMO (95)
30	400.0	0.0014	H-1→L+5 (88)
31	398.5	0.0052	H-6→LUMO (91)
32	398.0	0.0288	H-1→L+6 (49), HOMO→L+6 (24)
33	392.7	0.0543	H-2→L+5 (10), H-1→L+6 (25), HOMO→L+6 (34)
34	383.3	0.0001	H-4→L+5 (94)
35	383.0	0.0465	H-3→L+5 (14), H-2→L+5 (58)
36	377.0	0.6727	H-6→L+1 (11), H-3→L+5 (32), H-2→L+5 (15)
37	374.8	0.4934	H-6→L+1 (17), H-3→L+5 (36), H-2→L+5 (11)
38	374.1	0.174	H-7→LUMO (83), H-4→LUMO (13)
39	371.6	0.1713	H-2→L+6 (66)
40	367.0	0.0142	H-9→L+1 (23), H-6→L+1 (32), H-3→L+6 (26)
41	365.2	0.0758	H-9→L+1 (37), H-3→L+6 (36)

42	364.5	0.7481	H-6→L+2 (11)
43	362.7	0.0246	H-10→L+2 (33), H-10→L+3 (13), H-9→L+2 (11), H-8→L+2 (14)
44	361.2	0.0056	H-9→L+2 (21), H-9→L+3 (13), H-9→L+4 (14), H-6→L+2 (23)
45	359.5	0.0033	H-10→L+1 (10), H-10→L+3 (16), H-10→L+4 (20), H-5→L+6 (15)
46	359.0	0.0051	H-6→L+2 (13), H-5→L+6 (50)
47	357.5	0.6539	H-12→LUMO (13), H-6→L+1 (21), H-3→L+6 (13)
48	356.8	0.0159	H-12→LUMO (86)
49	355.1	0.4956	H-6→L+2 (40)
50	352.4	0.1716	H-6→L+3 (73)
51	348.4	0.006	H-6→L+4 (79)
52	346.8	0.0419	HOMO→L+7 (81)
53	344.4	0.0157	H-1→L+7 (63)
54	343.9	0.0491	H-13→L+1 (24), H-1→L+7 (23)
55	342.1	0.0249	H-13→L+2 (18), H-8→L+1 (25)
56	340.4	0.0284	H-11→L+2 (17), H-8→L+1 (12)
57	337.9	0.0246	H-11→L+1 (22), H-8→L+2 (19)
58	335.9	0.0606	H-14→L+1 (31), H-11→L+1 (25)
59	332.7	0.0525	H-14→L+2 (11), H-11→L+2 (36)
60	332.2	0.0035	H-15→L+2 (14), H-11→L+3 (18), H-8→L+2 (18)
61	331.3	0.0024	H-10→L+1 (37), H-9→L+1 (12), H-8→L+1 (20)
62	330.1	0.0269	H-13→L+1 (16), H-8→L+3 (10)
63	329.9	0.0281	H-13→L+2 (13), H-11→L+1 (11)
64	328.9	0.0051	H-5→L+5 (92)
65	328.3	0.0228	H-9→L+3 (10), H-2→L+7 (33)
66	328.1	0.0215	H-9→L+2 (25), H-9→L+3 (29), H-2→L+7 (19)
67	327.8	0	H-4→L+6 (100)
68	327.8	0.0439	H-11→L+4 (11), H-2→L+7 (32)
69	327.2	0.0473	H-11→L+4 (13), H-8→L+3 (18)
70	326.7	0.0011	H-10→L+2 (17), H-10→L+3 (18), H-10→L+4 (21), H-8→L+4 (13)
71	325.6	0.0033	H-9→L+3 (10), H-9→L+4 (37)
72	325.1	0.0064	H-14→L+1 (12), H-10→L+4 (12), H-9→L+4 (12)
73	324.0	0.0002	H-3→L+7 (95)
74	323.6	0.0004	H-15→L+2 (16), H-14→L+1 (13), H-13→L+2 (15)
75	322.6	0.01	H-14→L+2 (17), H-11→L+3 (11), H-11→L+4 (11), HOMO→L+8 (14)
76	321.8	0.0392	H-11→L+4 (12), HOMO→L+8 (60)
77	321.4	0.0006	H-16→L+1 (52), H-13→L+2 (14)
78	320.9	0.0034	H-15→L+1 (19), H-15→L+2 (12), H-15→L+3 (15), H-11→L+3 (11), HOMO→L+8 (13)
79	320.1	0.0134	H-14→L+3 (12), H-13→L+3 (46)
80	319.9	0.0002	H-7→L+1 (96)
81	319.3	0.0006	H-1→L+8 (75)
82	319.2	0.0001	H-8→LUMO (87)
83	318.7	0	H-9→LUMO (87)
84	318.4	0.0136	H-16→L+2 (12), H-16→L+3 (14), H-13→L+4 (30)
85	317.8	0	H-10→LUMO (94)

86	317.4	0.0013	H-16→L+2 (17), H-16→L+3 (10), H-14→L+3 (12), H-13→L+4 (23)
87	316.9	0.0365	H-15→L+1 (31), H-15→L+3 (20)
88	316.6	0.0229	H-13→L+4 (23), HOMO→L+9 (54)
89	316.1	0	H-13→LUMO (19), H-11→LUMO (73)
90	315.3	0.0064	H-16→L+2 (11), H-16→L+3 (17), H-14→L+2 (10), H-14→L+3 (18), H-14→L+4 (11), HOMO→L+9 (15)
91	315.2	0.0001	H-7→L+2 (98)
92	315.0	0	H-13→LUMO (69), H-11→LUMO (23)
93	314.6	0.0051	H-14→L+4 (20), H-1→L+9 (47)
94	313.9	0.0042	H-14→L+4 (42), H-1→L+9 (34)
95	313.2	0.0027	H-15→L+2 (15), H-15→L+3 (20), H-15→L+4 (42)
96	312.4	0.0058	H-16→L+4 (62)
97	312.1	0	H-7→L+3 (99)
98	311.9	0.0003	H-15→LUMO (13), H-14→LUMO (78)
99	311.8	0.0505	H-17→L+3 (13), H-17→L+6 (10), H-16→L+4 (16), H-5→L+7 (36)
100	309.5	0.8813	H-17→L+1 (16), H-6→L+5 (62)

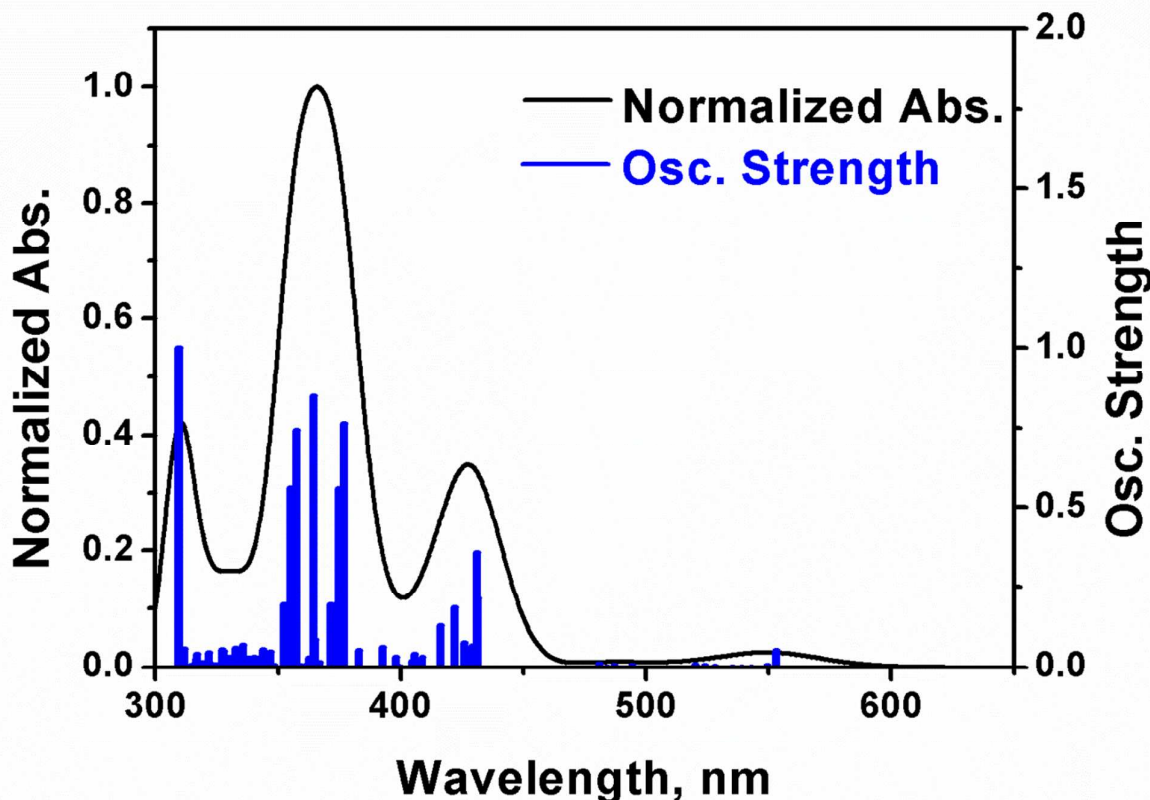


Figure S8. Bar graph reporting the calculated oscillator strength and calculated position of the 100st electronic transitions calculated by TDDFT for **1** (bar graph; f = computed oscillator strength). The black line is generated by assigning a thickness of 1000 cm⁻¹ to each bar.

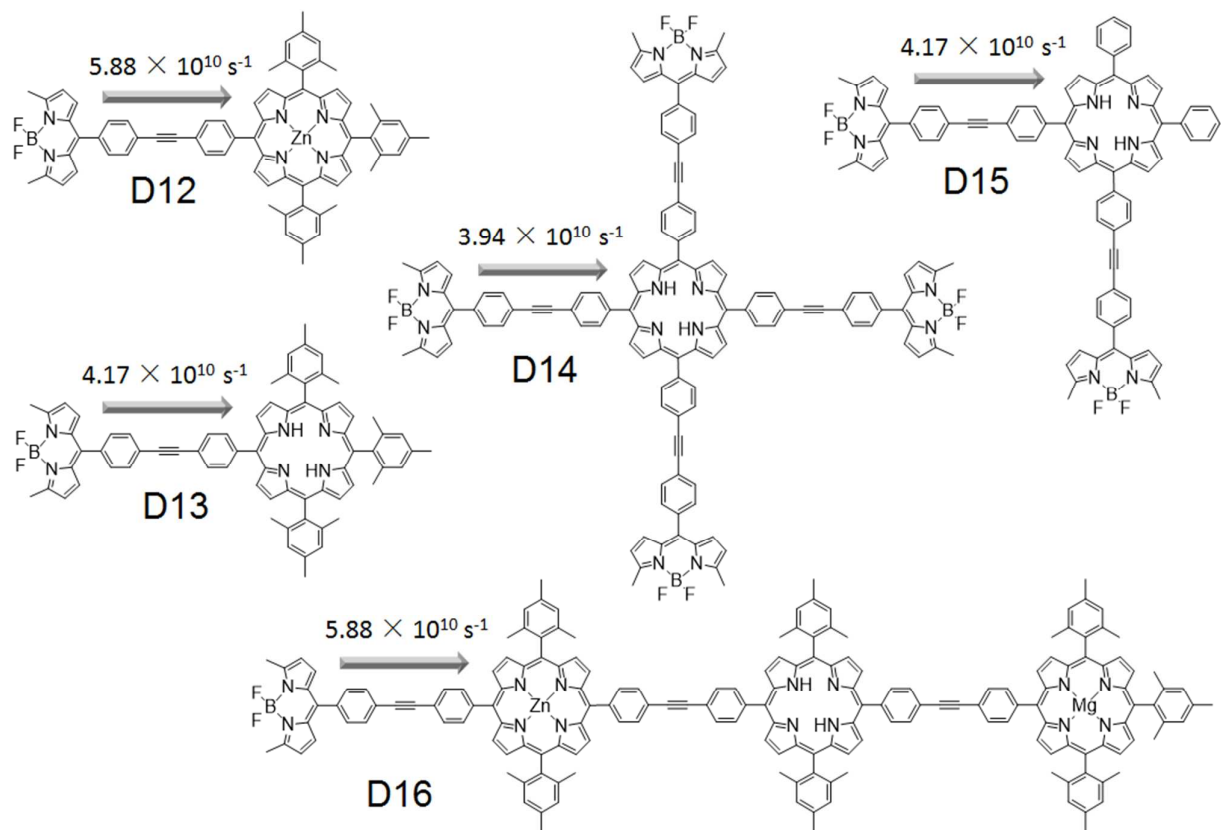
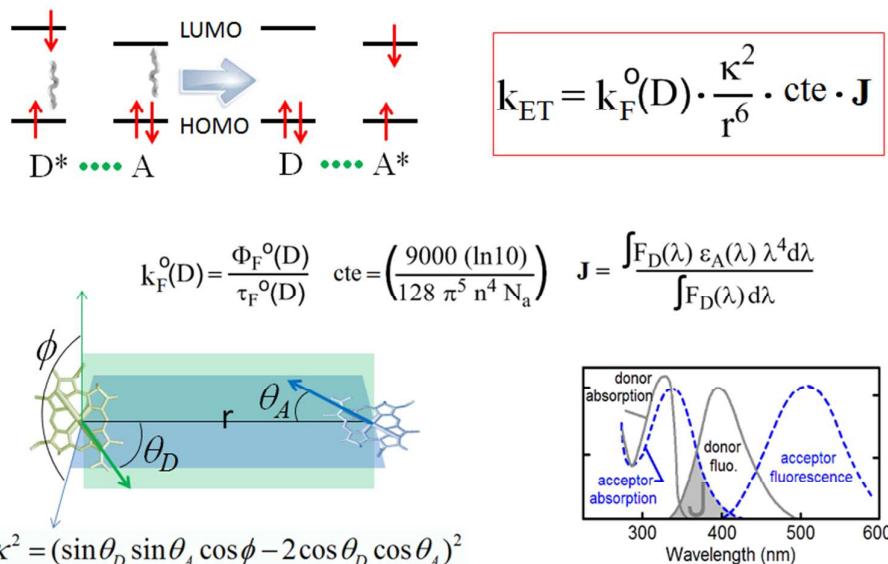


Figure S9. Comparison of $k_{\text{ET}}(\text{S}_1)$ for various literature dyads: **D12**^{S1} **D13**^{S1} **D14**^{S2} **D15**^{S2} and **D16**^{S3} at 298 K. Note that these dyads do not bare methyl groups at the β -position of [bod].

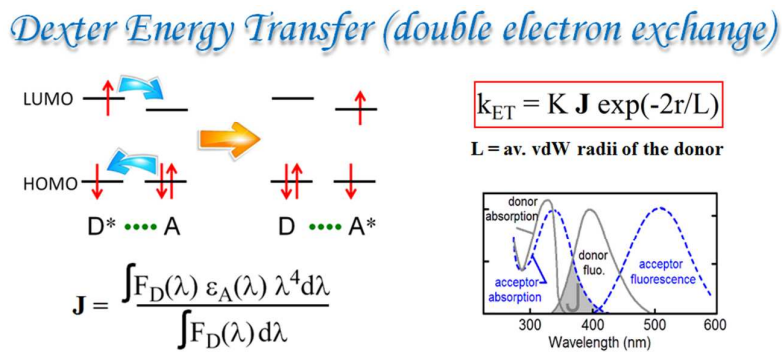
Förster Resonance Energy Transfer (FRET)



where D^* = donor in its S_1 excited state, A = acceptor, k_{ET} = rate for S_1 energy transfer, k_F^0 = fluorescence rate constant of the donor in the absence of energy transfer, κ^2 = orientation factor for the relative orientation of the transition moments of the donor and the acceptor (see green and blue arrows

on the left hand side at the bottom); this value can range between 0 (for perpendicular cases) and 4 (for parallel or anti-parallel cases), r = center-to-center separation between the donor and the acceptor, J = normalized J -integral, F_D = the fluorescence intensity (in wavelength scale), ε_A = absorptivity of the acceptor, n = average refractive index of the medium, and N_A = avogadro's number.

Figure S10. Description of the Förster's theory.^{S4}



where D^* = donor in its S_1 excited state, A = acceptor, k_{ET} = rate for S_1 energy transfer, K = a pre-exponential factor, r = center-to-center separation between the donor and the acceptor, L = average van der Waals radii of the donor, J = normalized J -integral, F_D = the fluorescence intensity (in wavelength scale), ε_A = absorptivity of the acceptor.

Figure S11. Description of the Dexter's theory.^{S5}

References

- (S1) Li, F.; Yang, S. I.; Ciringh, Y.; Seth, J.; Martin, C. H.; Singh, D. L.; Kim, D.; Birge, R. R.; Bocian, D. F.; Holten, D.; Lindsey, J. S. Design, Synthesis, and Photodynamics of Light-Harvesting Arrays Comprised of a Porphyrin and One, Two, or Eight Boron-Dipyrrin Accessory Pigments. *J. Am. Chem. Soc.* **1998**, *120*, 10001-10017.
- (S2) Kumaresan, D.; Datta, A.; Ravikanth, M. Photophysical Properties of Boron-Dipyrrin Appended Porphyrins with Heteroatom Cores. *Chem. Phys. Lett.* **2004**, *395*, 87–91.
- (S3) Lammi, R. K.; Wagner, R. W.; Ambroise, A.; Diers, J. R.; Bocian, D. F.; Holten, D.; Lindsey, J. S. Mechanisms of Excited-State Energy-Transfer Gating in Linear versus Branched Multiporphyrin Arrays. *J. Phys. Chem. B* **2001**, *105*, 5341-5352.
- (S4) Förster, T., Zwischenmolekulare Energiewanderung und Fluoreszenz. *Ann. Phys.* **1948**, *2*, 55-75.
- (S5) Dexter, D. L., A Theory of Sensitized Luminescence in Solids. *J. Chem. Phys.* **1953**, *21*, 836.